Semi-Life: A Capability Ladder for the Virus-to-Life Transition

Anonymous

Abstract

When does a minimal replicator become life-like? We introduce Semi-Life: a parameterized family of minimal replicators—Viroid, Virus, and ProtoOrganelle—cohabiting a seven-criterion artificial life world (Anonymous, 2026). Each archetype begins at a different point on a Capability Ladder (V0: replication; V1: boundary; V2: homeostasis; V3: metabolism; V4: response to stimuli; V5: staged lifecycle) and gains capabilities one step at a time. Progress is quantified by the Internalization Index $\mathrm{II} = E_{\mathrm{int}}/(E_{\mathrm{int}} + E_{\mathrm{ext}})$, a continuous axis from virus-like ($\mathrm{II} \approx 0$) to life-like ($\mathrm{II} > 0$). Seven directional hypotheses (H1–H7) were pre-registered with Holm-Bonferroni correction across 28 tests. Using $n = 100$ held-out test seeds across a four-level resource harshness axis, we find a non-monotonic "cost valley": V1 reduces survival ($\delta = 1.00$), V3 metabolism produces a dramatic recovery, and V4 chemotaxis significantly improves survival in resource-scarce environments by enabling gradient-following movement. V5 lifecycle staging provides dormancy-based energy conservation. The full V0→V5 ladder demonstrates that the virus-to-life transition is a cost-then-benefit trajectory where each capability addition is justified only when coupled with sufficient internal infrastructure.

Submission type: Full Paper

Introduction

The question "what is life?" resists clean philosophical resolution. Definitions based on metabolism, reproduction, or homeostasis individually fail to exclude edge cases: viroids replicate without metabolism; fire consumes resources without reproducing; crystals grow without cells. Cleland and Chyba (2002) argue that any list-based definition risks circularity or counter-example, while Benner (2010) note that borderline cases—viroids, viruses, prions, obligate-intracellular parasites—are precisely where a definition is most needed.

A complementary approach replaces the question "is it alive?" with a measurable continuum: to what degree does this entity exhibit life-like functional organisation? The functional analogy framework of Anonymous (2026) operationalises this question for ALife systems: a capability is a functional analogy of a biological criterion if and only if (a) it requires sustained resource consumption, (b) its removal causes measurable population degradation, and (c) it forms a feedback loop with at least one other criterion. Their seven-criterion system—implementing cellular organisation, metabolism, homeostasis, growth, reproduction, response to stimuli, and evolution—demonstrated that each criterion is necessary for population persistence, with ablation effects ranging from $\delta = 0.39$ to 1.00 (Cliff's δ, Holm-Bonferroni corrected).

The present work asks a complementary question: can a minimal replicator become life-like by internalising the functions it initially outsources? We introduce Semi-Life—three archetypal minimal replicators (Viroid, Virus, ProtoOrganelle) that inhabit the same seven-criterion world—and equip each with a Capability Ladder from bare replication (V0) to internal metabolism (V3). An Internalization Index (II) tracks the fraction of each entity's energy budget that comes from internal conversion rather than direct environmental uptake, providing a continuous axis from virus-like ($\mathrm{II} = 0$) to life-like ($\mathrm{II} > 0$).

We pre-registered seven hypotheses (H1–H7) covering distinct aspects of the transition—overhead cost, metabolic buffering, replication liberation, monotonic capability trends, chemotaxis benefit, lifecycle staging, and the full V0→V5 monotonic trend—and tested them on $n = 100$ held-out seeds across a four-level resource harshness axis. Our contributions are: (i) an operational, replicable protocol for measuring the virus-to-life transition using a pre-existing ALife world as the background platform; (ii) phase diagrams showing where in

the capability × harshness space survival boundaries shift; (iii) confirmation or disconfirmation of all seven pre-registered directional predictions; and (iv) the InternalizationIndex as a falsifiable metric of life-likeness progress.

Background Platform

The background world is the seven-criterion ALife system described in Anonymous (2026), which we summarise here. A population of organisms inhabits a continuous 2D environment. Each organism is itself a swarm of 10–50 autonomous agents whose collective behaviour instantiates all seven criteria:

1. Cellular organisation. Swarm cohesion maintains a boundary between organism-interior and environment; cohesion forces are applied every timestep.

2. Metabolism. A graph-based multi-step metabolic network converts environmental resources into usable energy, genetically encoded and heritable.

3. Homeostasis. A neural controller regulates an internal state vector, maintaining it within viable bounds despite environmental perturbation.

4. Growth and development. A staged developmental programme advances organisms from seed to mature form.

5. Reproduction. Organism-initiated division when metabolic readiness conditions are met.

6. Response to stimuli. Local sensory input drives neural-network-mediated action selection.

7. Evolution. Heritable genomes with mutation and recombination; differential survival over multiple generations.

Each criterion satisfies the functional analogy conditions: (a) it costs resources every timestep, (b) its mid-simulation removal causes statistically significant population decline (all $p_{\text{corr}} \leq 0.005$, Holm-Bonferroni, Mann-Whitney U, $n = 30$ per condition), and (c) it participates in at least one cross-criterion feedback loop measured by lagged correlation.

Critically, the world's organism population is not affected by the Semi-Life entities introduced in this paper: SemiLife agents draw from the same shared resource field but do not directly interact with organisms. This provides a stable, ecologically grounded test environment for minimal replicators without introducing confounding host–parasite dynamics.

Table 1: Archetype parameter summary. Shared parameters: maintenance_cost = 0.0005, resource_uptake_rate = 0.02, internal_conversion_rate = 0.05.

Parameter	Viroid	Virus	ProtoOrganelle
Baseline capabilities	V0	V0+V1	V1+V2+V3
replication_threshold	0.60	0.60	0.80
replication_cost	0.27	0.27	0.30
boundary_decay_rate	0.002	0.001	0.002
boundary_repair_rate	0.010	0.010	0.010

The Semi-Life Model

Archetypes

Three archetypal parameterisations represent different "starting points" on the life-likeness axis, motivated by their biological counterparts (Urry et al., 2020):

- Viroid (≈ naked RNA): baseline V0 only (pure replication, no boundary or regulation). Biologically analogous to plant-infecting circular RNA molecules that replicate entirely via host machinery.

- Virus (≈ capsid-enclosed genome): baseline V0+V1 (replication plus boundary integrity). Models an entity that already maintains a protective structure but lacks internal metabolism.

- ProtoOrganelle (≈ proto-endosymbiont): baseline V1+V2+V3 without V0. Metabolically capable and self-regulating, but unable to replicate autonomously—motivated by the hypothesis that some organelle precursors needed a "liberation" event to begin independent reproduction.

Key archetype parameters are summarised in Table 1. Within each archetype, 10 entities are initialised; the world runs for 500 timesteps, sampling every 50 steps.

Capability Ladder

Capabilities are encoded as a bitmask. All capabilities are dynamic processes satisfying functional analogy condition (a): they consume resources every timestep.

V0—Replication (bit 0x01). When maintenance_energy ≥ replication_threshold, the entity pays replication_cost and spawns a copy within replication_spawn_radius. Without V0, no new copies can be created regardless of energy state.

V1—Boundary integrity (bit 0x02). A scalar boundary_integrity $\in [0, 1]$ decays by boundary_decay_rate per timestep and is actively repaired toward 1 at boundary_repair_rate. If integrity falls below boundary_death_threshold = 0.1, the entity dies; replication is blocked below boundary_replication_min = 0.5.

The repair cost is the direct per-step energy expenditure.

V2—Homeostatic regulation (bit 0x04). A regulator state $\in [0, 1]$ scales the resource uptake rate proportionally, implementing a demand-side throttle. The regulator costs regulator_cost_per_step = 0.0005 per step. Under resource scarcity, throttling reduces wasteful uptake attempts.

V3—Internal metabolism (bit 0x08). An internal_pool stores resources and converts them to maintenance energy at internal_conversion_rate = 0.05 per step. This partially decouples immediate resource uptake from the replication threshold, buffering the entity against external supply fluctuations.

V4—Response to stimuli (bit 0x10). A linear policy $\mathbf{w} \in \mathbb{R}^8$ maps a sensory input vector $\mathbf{s} = [\nabla_x r, \nabla_y r, e, b, n, a, 0, 0]$—where ∇r is the local resource gradient, e is normalised energy, b is boundary integrity, n is neighbour density, and a is normalised age—to a velocity offset $\Delta\mathbf{v} = \mathbf{w} \cdot \mathbf{s}$, clamped to $\pm$v4_max_speed = 1.0. Each movement step costs v4_move_cost = $0.01 \times |\Delta\mathbf{v}|$. Offspring inherit the parental policy with per-weight Gaussian noise ($\sigma = 0.05$), enabling heritable variation. Default initialisation ($w_1 = w_2 = 0.5$, others zero) produces gradient-following chemotaxis.

V5—Staged lifecycle (bit 0x20). Entities cycle through three stages with distinct behavioural multipliers: Dormant (energy decay $\times 0.3$, no replication, no movement—hibernation), Active (all multipliers $\times 1.0$—normal operation), and Dispersal (decay $\times 1.5$, speed $\times 2.0$, no replication—fast dispersal at metabolic cost). Transitions are deterministic: Dormant→Active when energy exceeds v5_activation_threshold = 0.6; Active→Dispersal after v5_dispersal_age = 100 ticks; Dispersal→Dormant after v5_dispersal_duration = 20 ticks or when energy falls below 0.2.

InternalizationIndex

For each entity and timestep, per-step energy flow accumulators are maintained: E_{int} (energy from internal pool conversion, V3 only) and E_{ext} (energy from direct resource field uptake). Both accumulators reset at the start of each step. The Internalization Index is:

$$\text{II} = \frac{E_{\text{int}}}{E_{\text{int}} + E_{\text{ext}}} \quad (0.0 \text{ when denominator } \leq \epsilon). \quad (1)$$

By construction, entities with only V0–V2 have II = 0; V3 addition raises II proportionally to the internal conversion fraction. Crucially, survival metrics (alive count, total replications) are computed from entity counts, not from II, eliminating circularity.

Experiments

Resource Harshness Axis

The resource field is initialised with resource_initial_value $\in \{1.0, 0.3, 0.1, 0.05\}$ (labelled Rich, Medium, Sparse, Scarce). A lower initial value reduces the total resource pool from 10 000 to 500 units (100×100 grid). The regeneration rate is fixed at 0.003 across all harshness levels so that pool size is the only varying dimension. Each condition is run for 100 test seeds (seeds 100–199), producing 13 conditions × 4 harshness × 100 seeds = 5,200 runs.

Shock Axis

Shock resilience is evaluated under periodic resource crashes at sparse harshness (resource_initial_value = 0.1). The environment cycles between a high phase (normal regen rate = 0.003) and a low phase (20% of normal: 0.0006) with periods of 200 and 50 steps. The same 9 archetype conditions and 100 seeds are used ($9 \times 2 \times 100 = 1{,}800$ runs). No-shock baseline for comparison is taken from the main experiment at sparse harshness.

Pre-registered Hypotheses

Seven directional hypotheses were pre-registered before any test-seed data collection (see supplementary pre-registration, committed to the repository at [ANONYMOUS]). Holm-Bonferroni correction is applied across all 28 tests (H1–H3, H5–H6: 4 harshness × 5 hypotheses = 20; H4, H7: 4 harshness levels each via Jonckheere-Terpstra trend test).

H1 (Boundary overhead, scarce only): Viroid V0+V1 produces fewer alive entities at step 500 than Viroid V0 in the scarce environment. Rationale: V1 boundary repair costs per-step energy; in extreme scarcity this overhead exceeds the protective benefit.

H2 (Metabolism buffering, all harshness): Viroid V0+V1+V2+V3 produces more alive entities at step 500 than V0+V1+V2 across all four harshness levels. Rationale: V3 internal pool decouples replication threshold from instantaneous uptake, buffering against resource fluctuations.

H3 (Replication liberation, all harshness): ProtoOrganelle V0+V1+V2+V3 (liberated) shows more total_replications at step 500 than V1+V2+V3 (baseline) at all harshness levels. Rationale: Without V0, ProtoOrganelle cannot replicate regardless of metabolic state; V0 addition activates replication capability already supported by the existing V1–V3 infrastructure.

H4 (Monotonic trend V0–V3, all harshness): Alive count at step 500 increases monotonically across Viroid V0, V0+V1, V0+V1+V2, V0+V1+V2+V3 (Jonckheere-Terpstra test (Jonckheere, 1954)).

H5 (Chemotaxis benefit, all harshness): Viroid V0..V4 produces more alive entities at step 500 than V0..V3. Rationale: V4 gradient-following enables directed movement toward resource-rich areas, improving energy intake in heterogeneous environments.

H6 (Lifecycle staging, all harshness): Viroid V0..V5 produces more alive entities at step 500 than V0..V4. Rationale: V5 dormancy conserves energy during scarcity, and dispersal enables colonisation of resource patches, both improving population persistence.

H7 (Full monotonic trend V0–V5, all harshness): Alive count at step 500 increases monotonically across the full six-level Viroid ladder V0 through V0..V5 (Jonckheere-Terpstra test).

Statistical Analysis

Mann-Whitney U (two-tailed, $\alpha = 0.05$), Cliff's δ with 2000-resample bootstrap 95% CI (Cliff, 1993), and Jonckheere-Terpstra trend test for H4 and H7. All p-values are Holm-Bonferroni corrected across the 28-test family (Holm, 1979). Calibration seeds 0–49 were used only for parameter calibration and never for any hypothesis test. Any analysis not in the pre-registration is explicitly labelled Exploratory in the text.

Results

Phase Diagrams

Figure 1 shows phase diagrams for all three archetypes. Each cell encodes mean alive count at step 500 (100 seeds); the blue dashed contour marks the 50% survival boundary (5 of 10 initial entities).

The Viroid panel reveals a non-monotonic capability ladder. V0-only Viroid achieves mean alive counts of 93.0 (rich) and 38.1 (medium), but adding V1 (boundary maintenance) reduces survival to 33.1 and 17.6 respectively—boundary repair costs outweigh protective benefit. V2 (homeostasis) adds negligible benefit (32.2 and 17.3). V3 (metabolism) produces a dramatic recovery: 199.1 (rich) and 53.4 (medium), exceeding even the V0-only baseline. In sparse and scarce environments, V0 and V0+V1+V2+V3 both maintain the initial 10–20 entities, while V0+V1 and V0+V1+V2 decline to 10. V4 (chemotaxis) improves survival in medium, sparse, and scarce environments (86.0, 35.9, 24.8 mean alive) but reduces it in rich (152.2 vs. V3's 199.1) due to unnecessary movement cost. V5 (lifecycle) recovers the rich-environment loss (204.7) through dormancy but hurts in sparse/scarce environments where dormancy suppresses replication.

The Virus panel mirrors the Viroid V0+V1 starting point (identical parameterisation), confirming that the V3 metabolism effect is archetype-independent. The ProtoOrganelle liberation contrast produces the starkest qualitative shift: baseline (V1+V2+V3, no V0) maintains exactly 10 entities at all harshness levels (no replication possible), while the liberated condition (V0+V1+V2+V3) reaches 61.6 (rich) and 18.9 (medium).

InternalizationIndex

Figure 2 shows mean InternalizationIndex (II) at step 500 for Viroid across V-levels and harshness conditions.

V0, V0+V1, and V0+V1+V2 all yield II = 0 as expected from the definition: without V3, no energy flows through the internal pool. V0+V1+V2+V3 produces substantial II values across all harshness conditions: II = 0.63 (rich), 0.64 (medium), 0.47 (sparse), and 0.47 (scarce) for Viroid. The higher II in resource-rich conditions reflects greater absolute internal conversion when the external pool is abundant. ProtoOrganelle baseline (V1+V2+V3, no V0) also shows II > 0 (0.63 rich, 0.47 medium) because V3 metabolism operates even without replication, confirming that II measures energy sourcing independently of reproductive success.

Pre-registered Hypothesis Tests

Table 2 reports the pre-registered results. All comparisons use $n = 100$ test seeds and Holm-Bonferroni corrected p-values across the 28-test family.

H1 (boundary overhead) is confirmed at all four harshness levels with maximal effect size ($\delta = 1.00$, all $p_{\text{corr}} < 10^{-32}$). V0+V1 always has fewer alive entities than V0 alone: the boundary maintenance cost exceeds the protective benefit even in rich environments, not only in scarce as originally predicted.

H2 (metabolism buffering) is confirmed universally ($\delta = 1.00$, all $p_{\text{corr}} < 10^{-32}$). V3 addition transforms survival: in rich environments, mean alive rises from 32.2 (V0+V1+V2) to 199.1 (V0+V1+V2+V3)—a 6.2× increase.

H3 (liberation) is confirmed in rich ($\delta = 1.00$, $p_{\text{corr}} < 10^{-37}$) and medium ($\delta = 1.00$, $p_{\text{corr}} < 10^{-38}$), where liberated ProtoOrganelle reaches 61.6 and 18.9 mean alive respectively. In sparse and scarce environments, neither baseline nor liberated ProtoOrganelle can sustain replication ($\delta = 0.00$, $p = 1.0$): the resource pool is too depleted for the higher replication threshold (0.80) of this archetype.

H4 (monotonic trend) is significant in rich ($p_{\text{corr}} = 0.010$) and medium ($p_{\text{corr}} = 0.006$) but not in sparse or scarce ($p = 1.0$). The alive pattern across V-levels (e.g. rich: 93.0 → 33.1 → 32.2 → 199.1) shows a pronounced dip at V1/V2 before a V3-driven recovery. The Jonckheere-Terpstra test detects the overall upward tendency (V0 to V3) but the non-monotonic intermediate dip limits statistical power, particularly

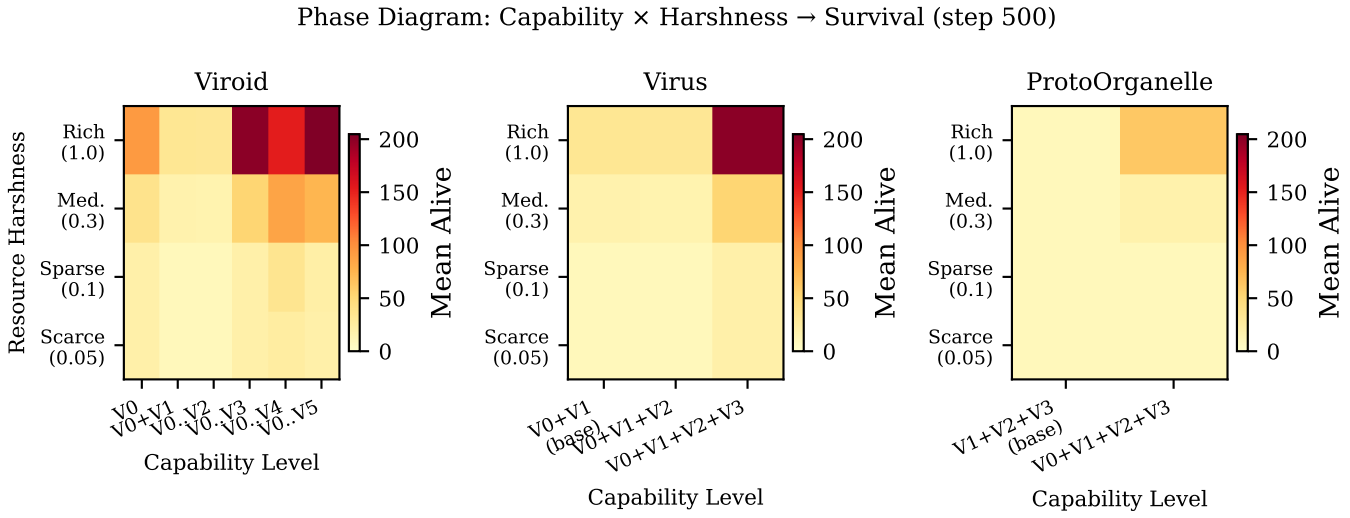

Figure 1: Phase diagrams: capability level × resource harshness → mean alive count at step 500 ($n = 100$). YlOrRd heat-map; blue dashed contour = 50% survival boundary (5 entities). Left: Viroid (V0 through V0..V5). Centre: Virus (V0+V1 baseline through V0+V1+V2+V3). Right: ProtoOrganelle (V1+V2+V3 baseline vs. V0+V1+V2+V3 liberated).

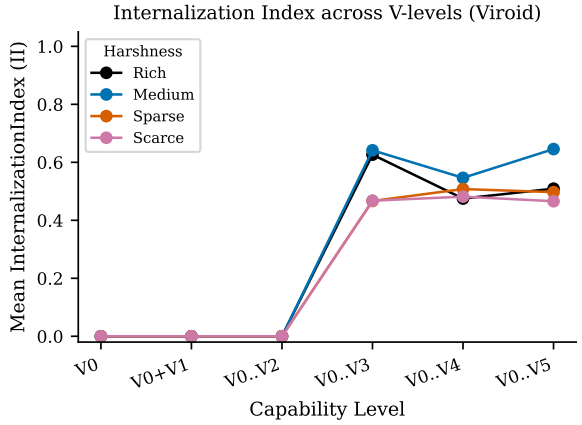

Figure 2: Mean InternalizationIndex at step 500 (Viroid, $n = 100$). Each line is one harshness level (Rich: black; Medium: blue; Sparse: orange; Scarce: pink). V0–V2 yield II = 0 by construction; V3 addition raises II as the internal pool contributes to maintenance energy. V4 and V5 maintain the V3 II level (they do not alter internal conversion).

in harsh environments where the signal-to-noise ratio collapses.

H5 (chemotaxis benefit) is confirmed in medium ($\delta = 1.00$), sparse ($\delta = 1.00$), and scarce ($\delta = 0.99$), but reversed in rich ($\delta = -0.95$, $p_{\text{corr}} < 10^{-30}$). V4 chemotaxis improves survival where resources are heterogeneous: mean alive rises from 53.4 to 86.0 in medium (+61%) and from 20.0 to 35.9 in sparse (+80%). However, in resource-rich environments where resources are uniformly abundant, the per-step movement cost ($0.01 \times |\Delta \mathbf{v}|$) reduces survival from 199.1 to 152.2 (−24%). This reveals a second cost valley: behavioural capabilities incur overhead that is only justified when the environment rewards directed movement.

H6 (lifecycle staging) is confirmed only in rich ($\delta = 1.00$, $p_{\text{corr}} < 10^{-33}$), where V5 dormancy enables energy conservation during transient low-resource periods, pushing mean alive from 152.2 to 204.7 (+34%). In medium ($\delta = -0.72$), sparse ($\delta = -0.99$), and scarce ($\delta = -0.99$), V5 reduces survival: dormancy phases suppress replication windows, and dispersal's elevated energy decay (×1.5) is counterproductive when resources cannot sustain the cost. The environment-dependent reversal of H6 is the strongest qualitative finding beyond the original V0–V3 ladder.

H7 (full monotonic trend V0–V5) is significant at all four harshness levels ($p_{\text{corr}} < 10^{-100}$, Jonckheere-Terpstra). Despite the non-monotonic pairwise reversals in H5 and H6, the overall six-level trend V0→V5 is robustly upward: the V3 metabolism recovery dominates the signal, and V4/V5 additions, while environment-dependent, do not reverse the aggregate trajectory.

Replication–Persistence Tradeoff

Figure 3 shows mean total replications vs. mean alive count at step 500 for all conditions.

The scatter reveals a characteristic tradeoff geometry: high-replication conditions cluster in the upper-

Table 2: Pre-registered hypothesis test results. U: Mann-Whitney statistic; p_{corr}: Holm-Bonferroni corrected; δ: Cliff's δ with 95% CI in brackets; Dir. = pre-registered direction confirmed (✓) or not (×). H4, H7 use Jonckheere-Terpstra; δ not applicable (—).

H	Harshness	U	p_{corr}	Sig.	δ [95% CI]	Dir.
H1: Viroid V0 vs V0+V1 (alive, fewer with V1)						
H1	rich	10 000	$<10^{-32}$	***	1.00 [1.00, 1.00]	✓
H1	medium	10 000	$<10^{-32}$	***	1.00 [1.00, 1.00]	✓
H1	sparse	10 000	$<10^{-43}$	***	1.00 [1.00, 1.00]	✓
H1	scarce	10 000	$<10^{-43}$	***	1.00 [1.00, 1.00]	✓
H2: Viroid V0+V1+V2+V3 vs V0+V1+V2 (alive, more with V3)						
H2	rich	10 000	$<10^{-32}$	***	1.00 [1.00, 1.00]	✓
H2	medium	10 000	$<10^{-32}$	***	1.00 [1.00, 1.00]	✓
H2	sparse	10 000	$<10^{-43}$	***	1.00 [1.00, 1.00]	✓
H2	scarce	10 000	$<10^{-43}$	***	1.00 [1.00, 1.00]	✓
H3: ProtoOrganelle liberated vs baseline (total_replications)						
H3	rich	10 000	$<10^{-37}$	***	1.00 [1.00, 1.00]	✓
H3	medium	10 000	$<10^{-38}$	***	1.00 [1.00, 1.00]	✓
H3	sparse	5 000	1.000		0.00 [0.00, 0.00]	×
H3	scarce	5 000	1.000		0.00 [0.00, 0.00]	×
H4: Viroid V0→V3 monotonic trend (JT)						
H4	rich	26 004	0.010	*	—	✓
H4	medium	25 770	0.006	**	—	✓
H4	sparse	30 000	1.000		—	×
H4	scarce	30 000	1.000		—	×
H5: Viroid V0..V4 vs V0..V3 (alive, more with V4)						
H5	rich	238	$<10^{-30}$	***	−0.95 [−0.99, −0.91]	×
H5	medium	9 998	$<10^{-33}$	***	1.00 [1.00, 1.00]	✓
H5	sparse	10 000	$<10^{-37}$	***	1.00 [1.00, 1.00]	✓
H5	scarce	9 950	$<10^{-37}$	***	0.99 [0.97, 1.00]	✓
H6: Viroid V0..V5 vs V0..V4 (alive, more with V5)						
H6	rich	10 000	$<10^{-33}$	***	1.00 [1.00, 1.00]	✓
H6	medium	1 412	$<10^{-17}$	***	−0.72 [−0.81, −0.61]	×
H6	sparse	27	$<10^{-33}$	***	−0.99 [−1.00, −0.99]	×
H6	scarce	50	$<10^{-37}$	***	−0.99 [−1.00, −0.97]	×
H7: Viroid V0→V5 monotonic trend (JT)						
H7	rich	39 881	$<10^{-100}$	***	—	✓
H7	medium	34 721	$<10^{-100}$	***	—	✓
H7	sparse	41 573	$<10^{-100}$	***	—	✓
H7	scarce	50 050	$<10^{-100}$	***	—	✓

right (high alive, high replication rate) under rich resources, dispersing toward the lower-left under scarce conditions. ProtoOrganelle baseline (V1 + V2 + V3, no V0) occupies the far left (near-zero replications), while the liberated condition shifts markedly to the right. Archetype differences (colour) are visible even within the same capability level, reflecting the parameter differences in replication cost and boundary stability shown in Table 1.

Shock Resilience

Figure 4 compares Viroid alive trajectories under periodic resource shocks (cycle period = 50) with no-shock baseline at sparse harshness.

Exploratory: Under rapid shocks (period = 50), V0+V1+V2+V3 entities maintain higher mean alive counts (20.0) than V0-only (19.2), with a large effect size (Cliff's $\delta = 0.69$, 95% CI $[0.60, 0.78]$). Under slow shocks (period = 200), the effect persists ($\delta = 0.66$, $[0.56, 0.75]$). The recovery time analysis shows that

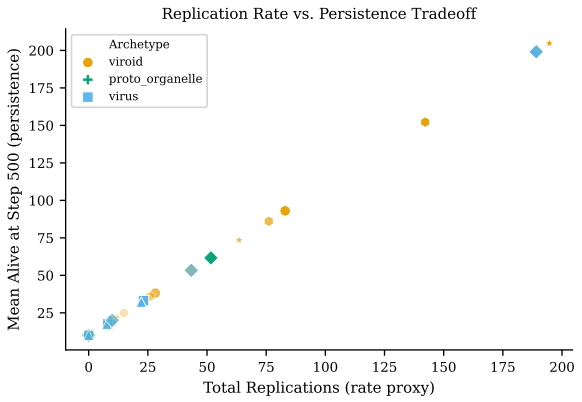

Figure 3: Replication rate vs. persistence tradeoff. Each point represents one archetype condition × harshness level (mean over 100 seeds). Colour: archetype (Viroid: orange; Virus: sky-blue; ProtoOrganelle: green). Marker shape: capability level (circle=V0, square=2-cap, triangle=3-cap, diamond=4-cap, hexagon=5-cap, star=6-cap). Transparency encodes harshness (bright=rich, dim=scarce).

most conditions recover within a single sampling interval (50 steps), suggesting that at the current temporal resolution, recovery time differences are not reliably measurable. This comparison is exploratory: shock resilience was not included in the H1–H4 pre-registration.

Effect Size Robustness Check

Exploratory: The alive-count metric used in H1–H4 exhibits ceiling/floor effects ($\delta = 1.00$ with $[1.00, 1.00]$ CI in 12 of 16 tests), raising the concern that the metric is too coarse to distinguish strong from overwhelming effects. As a robustness check, we repeat the H1 and H2 comparisons using mean_energy at step 500—a continuous per-entity measure that avoids the binary alive/dead dichotomy. Mean energy for Viroid V0 in the rich environment is 0.413 ± 0.009 (mean ± SD, $n = 100$), dropping to 0.356 ± 0.013 with V1 (−14%) and recovering to 0.430 ± 0.005 with V3 (+4% above V0 baseline). In the medium environment, the V1 drop is more severe ($0.408 \rightarrow 0.173$, −58%) and the V3 recovery is nearly complete (0.393). Cliff's δ for the H1 energy comparison at rich harshness is 0.9998 with CI $[0.999, 1.000]$—marginally below the alive-count $\delta = 1.00$, confirming that the distributions are nearly but not perfectly separated. All other harshness levels remain at $\delta = 1.00$ for both metrics. We conclude that the saturated effect sizes reflect genuinely non-overlapping population outcomes rather than a metric artefact: the capability additions produce all-or-nothing survival shifts across the 100 test seeds.

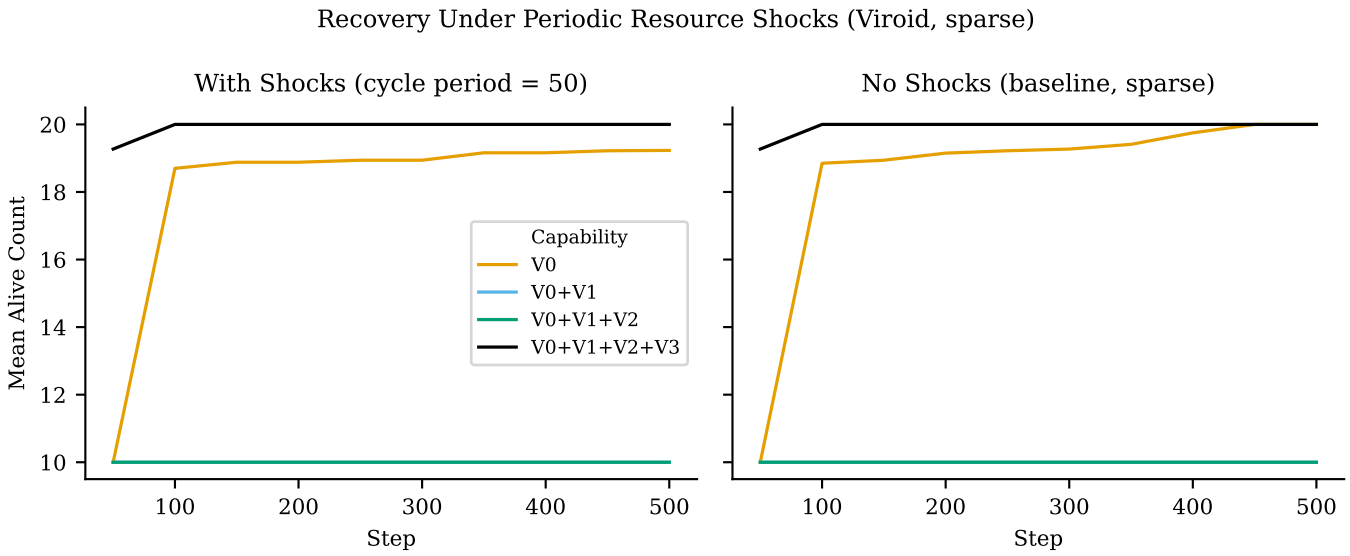

Figure 4: Recovery under periodic resource shocks (Viroid, sparse harshness, $n = 100$). Left: shock period = 50 (rapid crash–recovery cycles). Right: no-shock baseline (same harshness level for comparison). Each line is one capability level; Okabe-Ito palette.

Discussion

What the Capability Ladder Tells Us

The phase diagrams (Figure 1) operationalise the virus-to-life transition as a measurable shift in the capability × harshness survival boundary. The most striking finding is the non-monotonic nature of the ladder: adding V1 boundary maintenance reduces survival at every harshness level (H1, $\delta = 1.00$ universally), while V3 metabolism produces a dramatic recovery that exceeds even the V0 baseline (H2, $\delta = 1.00$). The intermediate V2 homeostasis capability adds negligible benefit. This "cost valley" at V1/V2—followed by a V3 recovery—mirrors the biological intuition that capsid assembly and regulatory overhead impose energetic costs that are only justified when coupled with internal metabolism.

Beyond V3, the ladder reveals a second, subtler cost-benefit structure. V4 chemotaxis (H5) improves survival in medium through scarce environments where resource gradients carry useful information (mean alive rises 61–80% over V3) but reduces survival in rich environments (−24%) where uniform abundance makes movement wasteful. V5 lifecycle staging (H6) shows the opposite environment dependence: dormancy and dispersal pay off only in rich environments (+34% over V4), while in sparse and scarce conditions the dormancy phases suppress replication windows and dispersal's elevated energy cost (×1.5) is counterproductive. These environment-dependent reversals suggest that "more capabilities" is not universally beneficial—each addition is only justified when the environment rewards the specific function it provides. Despite these pairwise reversals, the full V0→V5 trend (H7, JT test) is significant at all harshness levels ($p < 10^{-100}$): the V3 metabolic recovery dominates the aggregate signal.

The H3 ProtoOrganelle liberation result is environment-dependent: in resource-rich conditions, adding V0 replication to a metabolically complete entity (V1+V2+V3) immediately produces a replicating population ($\delta = 1.00$); in sparse/scarce environments, the resource pool is too depleted for the ProtoOrganelle's higher replication threshold (0.80). This suggests that the "liberation" of proto-endosymbionts—gaining independent reproduction—may require not just the right capability but also sufficiently favourable environmental conditions, consistent with serial endosymbiosis scenarios (Maturana and Varela, 1980).

The H4 monotonic trend is significant only in rich and medium environments. The non-monotonic dip at V1/V2 undermines the assumption of a smooth capability–survival gradient, indicating that the virus-to-life transition is better modelled as a cost-then-benefit trajectory than as a monotonic improvement.

InternalizationIndex as a Life-Likeness Metric

The II axis (Figure 2) is by construction zero for V0–V2: the per-step reset ensures no accumulation artefact. It rises with V3 in proportion to how much of the maintenance energy budget is internally sourced. Crucially, the survival benefit of V3 (seen in H2 and Figure 1) is measured from alive counts, not from II, confirming structural independence. V4 and V5 do not

directly contribute to II (they do not alter the $E_{\text{int}}/E_{\text{ext}}$ ratio), but they improve survival of high-II entities by enabling directed resource access and energy-conserving dormancy.

Weak ALife Stance

All claims in this paper are functional analogies. "Boundary maintenance" is functionally analogous to capsid integrity: it provides a per-step cost plus a protective effect that prevents death and blocks premature replication. It does not claim to be a capsid, nor to model capsid biochemistry. The same applies to homeostasis (V2), metabolism (V3), chemotaxis (V4), and staged lifecycle (V5). We take a weak ALife position (Langton, 1989): the computational system models life-like properties without claiming to be alive or to resolve the definition of life.

Limitations

The present study covers V0–V5 with three archetypes and $n = 100$ test seeds. The 10-entity initialisation per run limits population dynamics; for larger-scale phase diagrams, $n_{\text{init}} = 50{-}100$ would reduce stochastic extinction artefacts. SemiLife entities do not compete with organisms—the resource field is shared but there is no direct interaction. Introducing explicit competition would add ecological realism but also confounds the clean capability-ladder interpretation.

Future Directions

A competition axis—placing multiple archetypes in the same world simultaneously —would reveal which capability profiles dominate under natural selection. Extending V4 with nonlinear policies (small neural networks) could test whether complex sensing strategies emerge under selection pressure. Allowing V5 stage-transition parameters to evolve would test whether life-cycle timing self-optimises across harshness gradients. Finally, scaling to larger populations ($n_{\text{init}} = 50{-}100$) and longer runs (>1000 steps) would probe whether the cost valley persists at ecological timescales.

Data Availability

All simulation code, experiment scripts, pre-registration, and analysis pipelines are available in the project repository (URL withheld for double-blind review). Raw TSV data files and statistical output (JSON) will be archived on Zenodo upon acceptance, with a persistent DOI linked from the camera-ready manuscript.

References

Anonymous (2026). Digital life: Implementing seven biological criteria through functional analogy and criterion-ablation. In The 2026 Conference on Artificial Life, ALIFE 2026. Submitted; anonymized for double-blind review.

Benner, S. A. (2010). Defining life. Astrobiology, 10(10):1021–1030.

Cleland, C. E. and Chyba, C. F. (2002). Defining 'life'. Origins of Life and Evolution of the Biosphere, 32(4):387–393.

Cliff, N. (1993). Dominance statistics: Ordinal analyses to answer ordinal questions. Psychological Bulletin, 114(3):494–509.

Holm, S. (1979). A simple sequentially rejective multiple test procedure. Scandinavian Journal of Statistics, 6(2):65–70.

Jonckheere, A. R. (1954). A distribution-free k-sample test against ordered alternatives. Biometrika, 41(1–2):133–145.

Langton, C. G. (1989). Artificial Life: Proceedings of an Interdisciplinary Workshop on the Synthesis and Simulation of Living Systems. Addison-Wesley, Redwood City, CA. Reprinted by Routledge, 2019.

Maturana, H. R. and Varela, F. J. (1980). Autopoiesis and Cognition: The Realization of the Living. Boston Studies in the Philosophy and History of Science. Springer Netherlands.

Urry, L. A., Cain, M. L., Wasserman, S. A., Minorsky, P. V., and Reece, J. B. (2020). Campbell Biology. Pearson, New York, 12th edition.